Probability of path block by using microbubbles aggregation in artificial capillary

Kohji Masuda, Nobuhiko Shigehara, Ren Koda, and Takashi Mochizuki

Grad. School of Bio-Applications and Systems Eng.,
Tokyo Univ. of Agriculture and Technology, Koganei, Tokyo 184-8588 Japan
ultrason@cc.tuat.ac.jp
http://www.tuat.ac.jp/~masuda

Abstract. We have previously reported our attempts to produce microbubble aggregations, by making use of Bjerknes force, which acts to propel microbubbles and to adjust the size of aggregations. However, because we have used simple shape of artificial blood vessels, the behavior of aggregations in a capillary, e.g., probability to obstruct in bloodstream, possibility of embolization, has not been predicted. Thus we designed and fabricated a capillary-mimicking artificial blood vessel to apply to active path block with microbubble aggregation. The aggregation suddenly flaked off the vessel wall and flew to downstream, which was caught at a bifurcation with a high probability. We verified the same experiment under similar parameters to calculate the probability of path block.

1 Introduction

It is known that microbubbles form their aggregations by secondary acoustic force, which acts as attractive or repulsive force between the neighboring microbubbles, under ultrasound exposure. By making use of microbubble aggregations, the effects of ultrasound therapy would be expected by accelerating the temperature increase in thermal therapy [1,2] and inducing sonoporation [3] to allow the uptake of larger molecules into cells in physical drug delivery [4,5]. Though the mechanism to form aggregation is very complex, because of the connection among various parameters, various researches related to microbubble aggregations were experimentally and theoretically investigated [6-11]. However, the behavior of aggregations in a capillary, e.g., probability to obstruct in bloodstream, shape destruction of the aggregation, etc, has not been predicted. If there is a possibility that the aggregations might block vessels, it can be applied as a novel therapeutic method of an artificial embolization near the target area of a tumor.

We have ever reported our attempts to control microbubbles using the primary and secondary Bjerknes force to elucidate the conditions in sound pressure, central frequency of ultrasound, and flow velocity for active path selection in water flow [12,13] and trapping in blood flow [14] of microbubbles using artificial blood vessels with a simple shape. In those experiment we have experimentally found that there was an upper limitation of the size of microbubbles aggregations, which were propelled to the

wall by primary Bjerknes force, and finally they flaked off the wall and flied to downstream. Thus we have considered that it is important to confirm the behavior of the flown aggregations in a capillary in the lower course, before application to living organs. From this point of view, we executed to control the destination of microbubbles aggregations with the primary and secondary Bjerknes force with a capillary-mimicking artificial blood vessel. In this paper, we describe the experiments to investigate the probability of path block by the flown aggregations in an artificial capillary to evaluate the possibility for an artificial embolization.

2 Methods

An acoustic radiation force acts to propel an obstacle in the direction of acoustic propagation, which is proportion to the surface area of the obstacle. Thus if an aggregation of microbubbles can be regarded as a larger bubble, as shown in Fig.1, it would be easily propelled by less primary force. Thus it is very important to investigate behavior to form aggregations with various conditions of ultrasound.

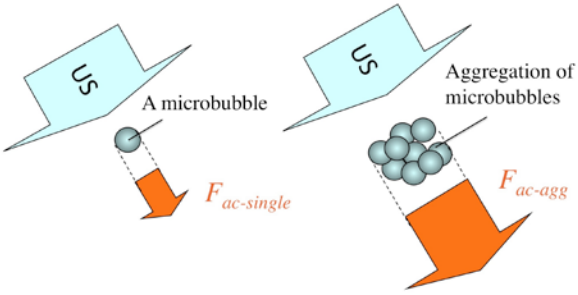

Fig. 1. Primary Bjerknes force to propel a microbubble and an aggregation along its direction of propagation.

2.1 Experimental setup

We used the microbubble Sonazoid®, which has a phospholipid shell and perfluorobutane inside with an average diameter in the range from 2 to 3 μm. The suspension of microbubbles was prepared just before the experiment at a concentration of 0.3 μL/kg, which was diluted 50 times from the original preparation of Sonazoid, because the diffusion in the human body was considered. To observe the behavior of the microbubbles, we have prepared transparent artificial blood vessels of capillary model made of the mixture material of wax and poly(vinyl alcohol) (PVA) by a fabrication method of grayscale lithography [15]. The inflow path of 2 mm was repeatedly divided into two lower courses to constitute the artificial capillary until the middle of the model, where the minimum diameter was 0.50 mm, as shown in Fig.2. After the middle of the model they converged toward the outflow of the model in the opposite way from the inflow to the middle. Fig.3 shows the experimental setup. It was fixedly

floated from the bottom of a water tank, which is filled with water, to prevent multiple reflections of ultrasound between the artificial blood vessel and the bottom of the tank. We used an optical microscope (Omron KH-7700) to observe the interested area in the blood vessel. The source of light is located above the water tank. The two-dimensional position of the blood vessel can be adjusted by an *x*-*y* stage. We used multiple ultrasound transducers including a concave ceramic disc to emit various frequencies of focused sinusoidal ultrasound. The transducers are to produce micro-bubbles aggregations in the middle of the path A.

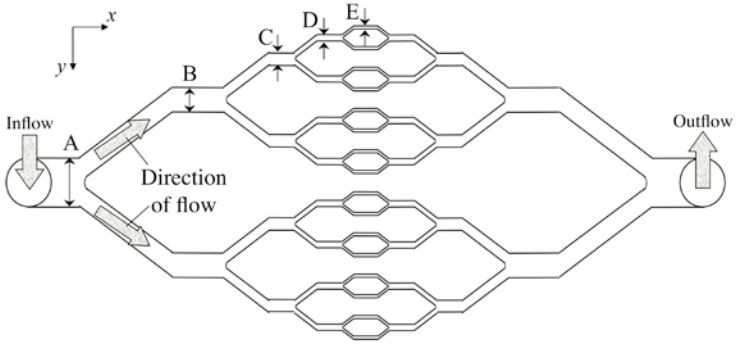

Fig. 2. Design of the artificial blood vessel of capillary model, where the diameters in A, B, C, D and E are 2.0, 1.4, 1.0, 0.7 and 0.5, respectively.

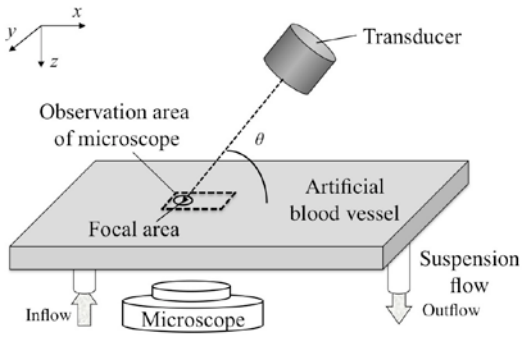

Fig. 3. Schematic of the experiment with the artificial blood vessel, the microscope and the ultrasound transducers.

2.2 Measurement of the size of aggregation

When the suspension of microbubbles was injected into the artificial blood vessel under continuous ultrasound emission, we have ever confirmed that cloudy aggregations of microbubbles were observed and varied according to conditions of the ultrasound, whereas no significant aggregations were observed in the case without ultrasound [14]. The size of an aggregation, which was considered to be sticking to the vessel wall, increases according to the time of ultrasound emission until it would flake

off the wall and fly to downstream. To evaluate the size of flown aggregations quantitatively, the straight path model is used. Fig.4 shows the procedure of the image processing to calculate the size of flown aggregations in the middle of the path, where the flow velocity was 20 mm/s in this case. The microscopic image was continuously recorded as a video file from the beginning of the experiment. Then the area of aggregation was calculated by subtracting from the initial image. Because the moment when the aggregation flies to downstream cannot be predicted, duration of ultrasound emission is set up to 30 s, in which condition the growth of aggregation can be observed. The subtraction image was converted to a gray scale image for application to unsharp masking for edge enhancement of the aggregations. Finally calculating the binary image by discriminant analysis method [14], the size of flowed aggregations is obtained.

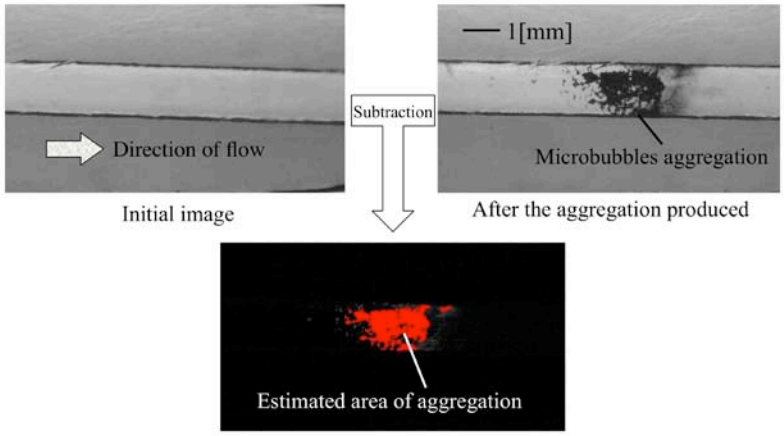

Fig. 4. Measurement of the size of flown aggregation in the middle of the path.

3 Results

3.1 The size of aggregation

As mentioned in the previous section, the size of aggregation was measured by using the straight path model before applying the artificial capillary. The focal area of sound field was set in the path A in Fig.2. The angle of the axis of the transducer was set at θ = 60 degree to avoid physical interference of both the source of light and the edge of the tank. The central frequencies of continuous wave emitted \were ranged in 3, 5, 7, 10 MHz to compare the dependence of frequency.

We examined the experiment with the parameters of flow velocity, maximum sound pressure, central frequency and duration of ultrasound emission. The size of microbubble aggregation increases according to the exposure time of ultrasound emission, where the several small aggregations were gradually coalesced. Fig.5 and 6 show the

measured size of aggregation versus central frequency and flow velocity, respectively, when the duration of ultrasound emission was 30 sec and the maximum sound pressure was 300 kPa-pp. In Fig.5, flow velocity was fixed as 20 mm/s. We have confirmed that the central frequencies of 5 and 7 MHz were appropriate to form aggregation with the microbubbles we used. In Fig.6, central frequency was fixed as 5 MHz. When flow velocity was 10 mm/s, the density of microbubbles was not enough to form aggregation. When flow velocity was 60 mm/s, on the other hand, microbubles cannot stick on the vessel wall due to flow resistance.

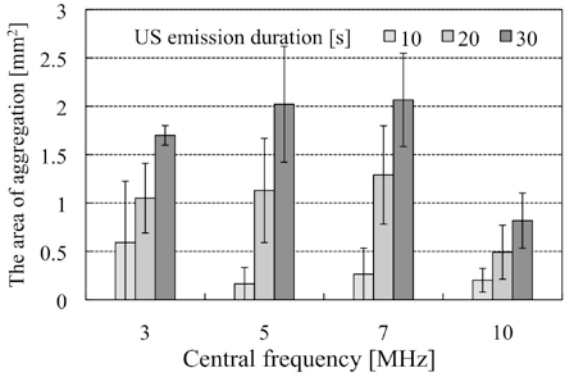

Fig. 5. The area of aggregation versus central frequency of ultrasound emission with flow velocity of 20 mm/s with sound pressure of 300 kPa-pp.

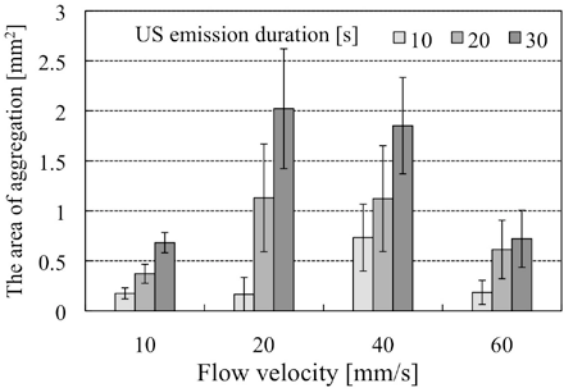

Fig. 6. The area of aggregation versus flow velocity with central frequency of 5 MHz with sound pressure of 300 kPa-pp.

3.2 Probability of path block

We have investigated the probability of path block. From the results in the previous section, we selected the parameters of the central frequency of 5 MHz and sound

pressure of 300 kPa-pp. Fig.7 shows the successive microscope images of the observation area after ultrasound emission was started, at flow velocity of 20 mm/s. Duration of ultrasound emission was 30 s. In 33.9 s after the injection of the suspension (3.9 s after stopping the emission), microbubbles aggregation was flaked off the vessel wall and appeared in the observation area. In 36.1 s the aggregation was caught at a bifurcation between the paths of C and D. Because the flown aggregation stayed for more than 20 s, finally we have injected colored water on behalf of the suspension. It was clearly confirmed that the aggregation blocked the path, where colored water could not penetrate to downstream.

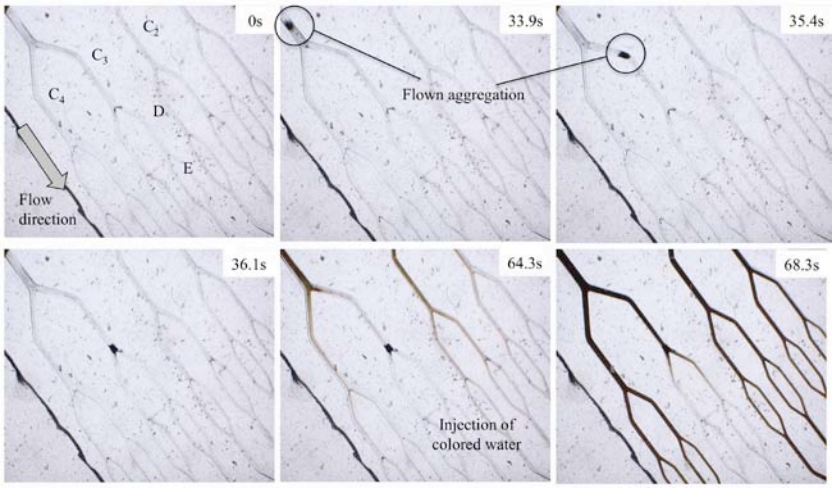

Fig. 7. Successive microscopic images near the paths of C, D and E after microbubbles suspension was injected when the standing wave at the point R was switched off.

We verified the same experiment under similar parameters, with duration of ultrasound emission was set to 10, 20 and 30 s. The probability of path block, which was calculated by dividing the success number of path block by the number of attempts (30 times), was calculated as Fig.8. In this graphs "Through" means that path block was not confirmed in all paths. The probability of path block increased with emission duration of ultrasound, inversely with flow velocity.

To apply this technique for an actual treatment, acoustic radiation force should be produced by plane wave, not by focused wave, to cover multiple capillaries in an internal organ to produce the asymmetry of distribution of microbubbles, where more amount of microbubbles are concentrated near target treatment area.

4 Conclusions

In this study, we have investigated the influence of the flown aggregations using an artificial capillary. First we estimated the sizes of flown aggregation. Second we investigated the probability of path block in the capillary model, where the sizes of flown aggregation were expected greater than the section area of the minimum path.

Because we showed very preliminary results in this paper, we are going to investigate with more kinds of parameters to enhance the possibility of artificial embolization.

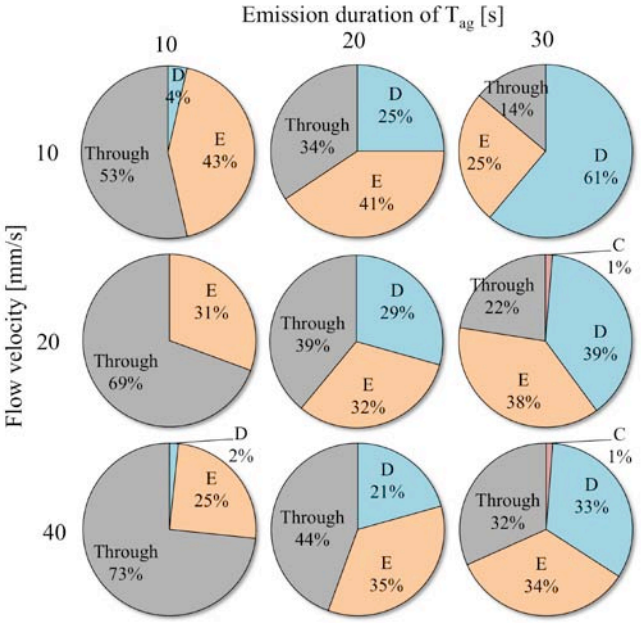

Fig. 8. The probability of path block with the locations where microbubbles aggregation was trapped in.

References

1. E. Stride and N. Saffari: Ultrasonics 42 (2004) 907.
2. G. J. Liu, F. Moriyasu, T. Hirokawa, et al: Ultrason. Med. Biol. 36 (2010) 78.
3. K. Osawa, Y. Okubo, K. Nakao, N. Koyama, and K. Bessho: J. Gene Med. 11 (2009) 633.
4. N. Kudo, K. Okada, and K. Yamamoto: Biophys. J. 96 (2009) 4866.
5. L. J. M. Juffermans, A. van Dijk, C. A. M. Jongenelen, et al: Ultrason. Med. Biol. 35 (2009) 1917.
6. Y. Yamakoshi and T. Miwa: Jpn. J. Appl. Phys. 50 (2011) 07HF01.
7. V. Garbin, M. Overvelde, B. Dollet, et al: Physics in Medicine and Biology 56 (2011) 6161.
8. S. Kotopoulis and M. Psotema: Ultrasonics 50 (2010) 260.
9. Y. Yamakoshi and T. Miwa: Jpn. J. Appl. Phys. 47 (2008) 4127.
10. Y. Matsumoto and S. Yoshizawa: Int. J. Num. Meth. Fluids 47 (2005) 591.
11. N. A. Pelekasis, A. Gaki, A. Donikov, and J.A. Tsamopoulos: J. Fluid Mechanics 500 (2004) 313.
12. K. Masuda, Y. Muramatsu, S. Ueda, et al: Jpn. J. Appl. Phys. 48 (2009) 07GK03.
13. K. Masuda, N. Watarai, R. Nakamoto, and Y. Muramatsu: Jpn. J. Appl. Phys. 49 (2010) 07HF11.
14. K. Masuda, R. Nakamoto, N. Watarai, et al: Jpn. J. Appl. Phys. 50 (2011) 07HF11.
15. T. Nakano, K. Yoshida, S. Ikeda, et al: Proc. IEEE IROS, 2009, p. 75.